SF2A 2011
G. Alecian, K. Belkacem, R. Samadi and D. Valls-Gabaud (eds)

SPITZER CHARACTERIZATION OF DUST IN THE IONIZED MEDIUM OF THE LARGE MAGELLANIC CLOUD

D. Paradis[1,2,3], R. Paladini[3], A. Noriega-Crespo[3], G. Lagache[4], A. Kawamura[5], T. Onishi[6] and Y. Fukui[5]

Abstract. Dust emission associated with ionized gas has so far been detected only in our Galaxy, and for wavelengths longer than 60 μm. Spitzer data now offer the opportunity to carry out a similar analysis in the Large Magellanic Cloud, and to separate dust emission into components associated with different phases of the gas, i.e. atomic, molecular and ionized. We perform a correlation study using infrared Spitzer data as part of the Surveying the Agents of a Galaxy's Evolution (SAGE) and IRAS 12-100 μm combined with gas tracers such as the ATCA/Parkes HI data, for the atomic phase, the NANTEN ^{12}CO data, for the molecular phase, and both the SHASSA Hα and the radio Parkes 5 GHz data, for the ionized phase. In particular, we investigate the presence of dust for different physical regimes of the ionized gas, spanning emission measures from 1 pc cm^{-6} (diffuse medium) to 10^3 pc cm^{-6} (HII regions).

Keywords: dust, extinction, HII regions, Magellanic Clouds

1 Introduction

The Large Magellanic Cloud (LMC), located at a distance of 50 kpc has an advantageous almost face-on viewing angle, with small contamination along the line of sight (LOS). Assessing the presence of dust in the ionized gas phase is very important given that the optical properties of dust grains can vary with the properties of the local environment. In the ionized medium, due to the proximity of the ionized gas with UV sources, such as O and B stars, and the cumulative effect of shock fronts, changes in the optical dust properties are indeed expected. For instance, depletion of polycyclic aromatic hydrocarbons (PAHs) has been observed towards individual HII regions. However, this phenomenon does not appear to be systematic. We present a systematic investigation of the dust properties associated with the ionized gas in the LMC. The full description of this analysis is presented in Paradis et al. (2011a).

2 Data

We use the following data set:

- Infrared: Spitzer data as part of the SAGE program (Meixner et al. 2006), from 3.6 to 160 μm, combined with IRAS 12-100 μm ($4'$ angular resolution).
- HI: 21 cm integrated intensity map (W_{HI}), obtained from the combined ATCA ($1'$ Kim et al. 2003) and Parkes data ($4'$ Staveley-Smith et al. 2003). Assuming the gas is optically thin, we derive: $N_H = 1.82 \times 10^{18} W_{HI}$.

[1] Universite de Toulouse; UPS-OMP, IRAP, Toulouse, France
[2] CNRS; IRAP, 9 av. du Colonel Roche, BP 44346, 31028, Toulouse, cedex 4, France-Spitzer Science CEnter, California Institute of Technology, 1200 E. California Blvd, Pasadena, CA 91125, USA
[3] Spitzer Science Center, California Institute of Technology, 1200 E. California Blvd, Pasadena, CA 91125, USA
[4] Institut d'Astrophysique Spatiale, 91405 Orsay, France
[5] Department of Astrophysics, Nagoya University, Chikusa-ky, Nagoya 464-8602, Japan
[6] Department of Physical Science, Osaka Prefecture University, Gakuen 1-1, Sakai, Osaka 599-8531, Japan

- CO: ^{12}CO(J=1-0) integrated intensity map (W_{CO}), second survey (2.′6, Fukui et al. 2008) obtained with the 4-m radio NANTEN telescope. We compute $N_H = 2X_{CO}W_{CO}$, using X_{CO} values deduced from virial masses for each cloud (Fukui et al. 2008).

- Hα: SHASSA survey (Gaustad et al. 2001), with an angular resolution of 0.′8. We compute $N_H = 1.37 \times 10^{18}\, I_{H\alpha}\, n_e$ (assuming 1R corresponds to an emission measure of 2.25 cm^{-6} pc.

- Radio at 5 GHz: Parkes data at a resolution of 5.′6 (Filipovic et al. 1995). The data are transformed in Hα emission using: $T_b/I_{H\alpha} = 8.396 \times 10^3 \nu_{GHz}^{2.1} T_4^{0.667} 10^{0.029/T_4}(1 + 0.008)$ (Dickinson et al. 2003).

3 Regimes of the ionized gas

We consider three regimes of the ionized gas, from diffuse H$^+$ to bright HII regions, determined using the pixel brightness distribution of the SHASSA map and the Kennicutt & Hodge (1986) catalog of HII regions:

- Case1: diffuse ionized gas 0.8 R $<$ Hα $<$ 7 R, $n_e = 0.055$ cm^{-3} (intermediate value from Haffner et al. (2009))

- Case 2: typical HII regions 7 R $<$ Hα $<$ 106 R, we derived $n_e = 1.52$ cm^{-3}

- Case 3: bright HII regions 106 R $<$ Hα $<$ 1000 R, we derived $n_e = 3.98$ cm^{-3}

4 Extinction in bright HII regions

The comparison between the SHASSA map and the Parkes data (converted to Hα emission) highlights that for 88% of pixels of case 3, the Hα-Parkes data are higher than the SHASSA ones, with a median ratio equal to 1.6. To explain such a discrepancy, we invoke extinction as a source of attenuation in the SHASSA map. In our analysis, the factor 1.6 of discrepancy would induce an extinction value in the SHASSA map of 0.51 mag in bright HII regions. Following O′Donnell (1994), Dickinson et al. (2003) estimate the absorption in the Hα as $A(H\alpha) = 0.81A(V)$. The corresponding extinction of LMC bright HII regions in the visible is A(V)=0.63 mag.

5 Decomposition of the IR emission and modeling

In the LMC, Bernard et al. (2008) evidenced the existence of a large FIR excess with respect to the atomic, molecular and ionized gas phases, which they attributed to either molecular gas with no associated CO emission or to optically thick HI. Following Paradis et al. (2011b), we decompose the IR emission at each wavelength and for each regime, as a function of the atomic, molecular and ionized gas column density:

$$I(\lambda) = a(N_H^{HI} + N_H^{X}) + bN_H^{CO} + cN_H^{H+} + d \tag{5.1}$$

with $\mathrm{N_H^X}$ the column density in the FIR excess component. In the following, we refer to the sum of the atomic and FIR excess components as the atomic phase.

The Hα map is used for the three regions as a tracer of the H$^+$ column density, whereas radio map at 5 GHz is used only for case 3 due to its lower sensitivity.

The thermal fraction of the 5 GHz map ($\mathrm{f_{th}}$) has been estimated, using:

$$\frac{S_5}{S_{1.4}} = f_{th}\left(\frac{\nu_5}{\nu_{1.4}}\right)^{-\alpha_{ff}} + (1 - f_{th})\left(\frac{\nu_5}{\nu_{1.4}}\right)^{-\alpha_{sync}} \tag{5.2}$$

where $\mathrm{S_5}$ and $\mathrm{S_{1.4}}$ are the total flux densities at 5 and 1.4 GHz, and α_{ff} and α_{sync} are the free-free and synchrotron spectral indices, taken equal to 0.1 and 0.6 respectively. We derive an average thermal fraction of 0.85 in bright HII regions of the LMC.

First, we assume a single radiation field along the LOS. We model the spectral energy distributions (SEDs) associated with each phase of the gas using DustEM (Compiègne et al. 2011, see Fig. 2). We impose, for dust emission associated with the atomic and molecular phases, as well as for dust emission associated with the diffuse ionized gas in case 1, the same interstellar radiation field (RF) hardness as for the solar neighborhood (Mathis et al. 1983). However for cases 2 and 3, dust in the ionized phase is associated with typical and bright

HII regions, and therefore it is essentially heated by local hot stars. For these cases, using the GALEV code*, we have generated an UV/visible spectrum of young stellar clusters of 4 Ma. Second, we test our results using a combination of several RF intensities and hardnesses along the LOS. For this purpose we apply the Dale et al. (2001) model that considers a local SED combination by assuming a power-law distribution of dust mass subjected to a given heating intensity.

6 Results

We evidence for the first time dust emission associated with the ionized gas of the LMC. We report:

- A systematic warmer dust temperature in the H^+ phase compared to the HI and CO phases
- An emissivity in the diffuse H^+ of 2.3×10^{-26} cm^2/H at 160 μm, lower than Galactic values by a factor higher than the metallicity ratio between the two galaxies. This result suggest different properties of dust in the H^+ gas of the LMC, compared to our Galaxy.
- A significant decrease of the PAH relative abundance in the H^+ phase of all cases (1, 2, 3) with respect to the HI and CO phases, with a larger difference between the phases for cases 2 and 3. We interpret this result as due to PAH destruction caused by the increased radiation field in the H^+ phase, although the origin of this phenomenon is still under investigation.
- The survival of the PAHs in the molecular phase. In addition, when one compares bright with typical HII regions, the H^+ phase shows an enhancement of the very small grains relative abundance by more than a factor of 2.
- An important increase of a near-infrared continuum in the H^+ phase, which does not seem to correlate with PAH emission.
- A systematic increase of the dust emission going from the diffuse medium to bright HII regions, for all gas components.

References

Bernard, J.-P., et al. 2008, ApJ, 136, 919
Compiègne, M., et al. 2011, A&A, 525, 103
Dale, D. A., et al. 2001, ApJ, 549, 215
Dickinson, C., Davies, R. D., and Davis, R. J. 2003, MNRAS, 341, 369
Filipovic, M. D. et al. 1995, A&AS, 111, 311
Fukui, Y., et al. 2008, ApJS, 178, 56
Gaustad, J. E., McCullough, P. R., Rosing, W., & van Buren, D. 2001, PASP, 113, 1326
Haffner, L. M., et al. 2009, RvMP, 81, 969
Kennicutt, R. C., & Hodge, P. W. 1986, ApJ, 306, 130
Kim, S., et al. 2003, ApJS, 148, 473
Mathis, J. S., Mezger, P. G., & Panagia, N. 1983, A&A, 128, 212
Meixner, M., et al. 2006, AJ, 132, 2268
O'Donnell, J. E. 1994, ApJ, 422, 158
Paradis, D. et al. 2011a, ApJ, 735, 6
Paradis, D. et al. 2011b, AJ, 141, 43
Staveley-Smith, L., et al. 2003, MNRAS, 339, 87

*available at `http://www.galev.org`

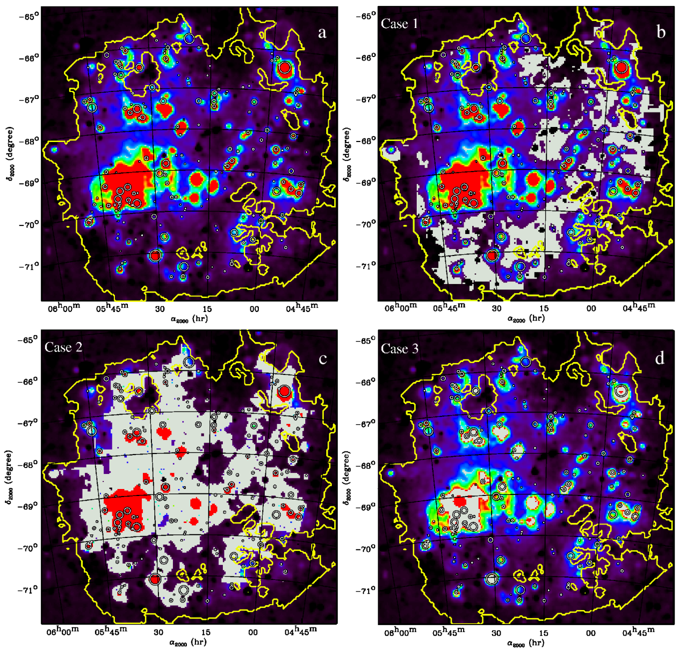

Fig. 1. SHASSA Hα map (*a*) and spatial locations of pixels (in gray) selected for each case: (*b*) case 1 (diffuse ionized gas), (*c*) case 2 (typical HII regions), and (*d*) case 3 (bright HII regions). The overlaid symbols show the HII regions (Kennicutt & Hodge 1986). The range of the maps is [-8; 100] R.

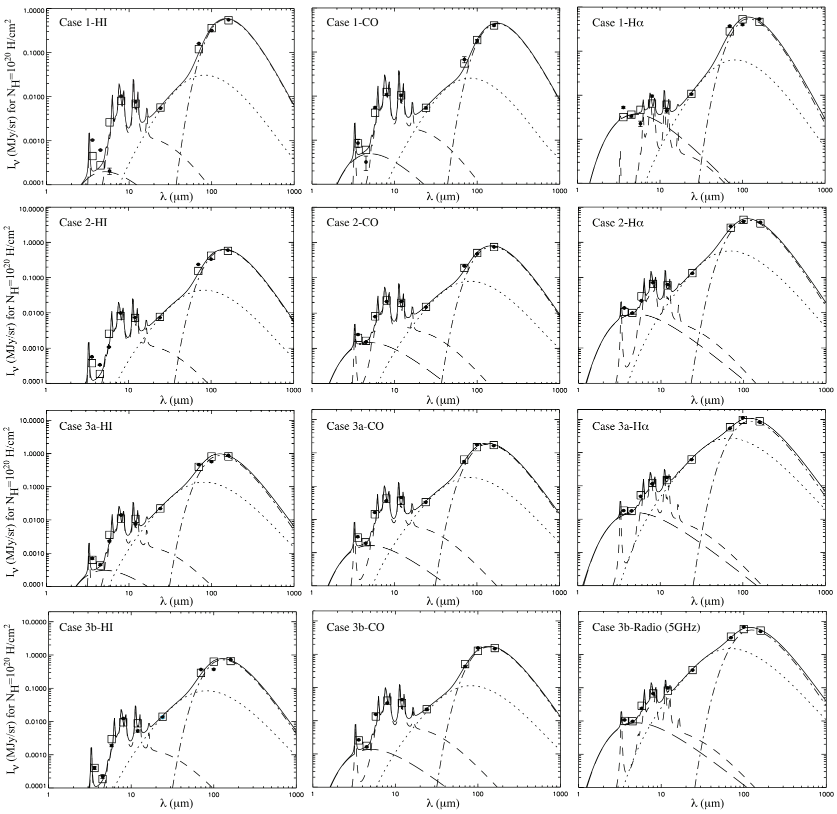

Fig. 2. Results of the fits obtained with the dust emission model (DustEM) assuming a single RF along the LOS. The squares show the fits of the model after applying the color-correction. Different curves denote the contributions from various grain populations: total (solid), big grains (dot-dash), very small grains (dot), polycyclic aromatic hydrocarbons (dash) and a near-infrared continuum (long dash).